Design and Construction of a PET-Compatible Double-Tuned $^{1}H/^{31}P$ MR Head Coil

A. Avdo Celik, Chang-Hoon Choi, Lutz Tellmann, Claire Rick, N. Jon Shah, and Jörg Felder,
Member, IEEE

***Abstract*—Simultaneous MR-PET is an increasingly popular multimodal imaging technique that is able to combine metabolic information obtained from PET with anatomical/functional information from MRI. One of the key technological challenges of the technique is the integration of a PET-transparent MR coil system, a solution to which is demonstrated here for a double-tuned $^{1}H/^{31}P$ head coil at 3 T. Two single-resonant birdcage coils tuned to the ^{1}H and ^{31}P resonances were arranged in an interleaved fashion and electrically decoupled with the use of trap circuits. All high 511 keV quanta absorbing components were arranged outside the PET field-of-view in order to minimize count rate reduction. The materials inside the PET field-of-view were carefully evaluated and chosen for minimum impact on the PET image quality. As far as possible, the coil case was geometrically optimized to avoid sharp transitions in attenuation, which may potentially result in streaking artefacts during PET image reconstruction. The coil caused a count rate loss of just above 5% when inserted into the PET detector ring. Except for the anterior region, which was designed to maintain free openings for increased patient comfort, an almost uniform distribution of 511 keV attenuation was maintained around the circumference of the coil. MR-related performance for both nuclei was similar or slightly better than that of a commercial double-tuned coil, despite the MR-PET coil having a close-fitting RF screen to shield the PET and MR electronics from possible electromagnetic interferences.**

***Index Terms*—$^{1}H/^{31}P$, double-tuned RF coil, low count-rate loss, simultaneous PET-MR**

I. Introduction

The use of MRI and PET as stand-alone imaging modalities is now considered to be standard in routine clinical practice, with MRI primarily being used to generate structural/anatomical images and PET being used to identify metabolic changes. However, recent technological advances have made the combination of these modalities into a single imaging system increasingly advantageous. In addition, interest and developments in the use of so-called 'X-nuclei' such as sodium-23 (^{23}Na) or phosphorus-31 (^{31}P), for use alongside ^{1}H proton imaging, as potential biochemical markers in MR, are also increasing [1]. In this context, integrated MR-PET systems that allow simultaneous multimodal data acquisition are favored as physiological processes can be investigated concurrently with MR and PET. Consequently, the use of a double resonant head-coil capable of operating inside a PET detector ring while maintaining good signal-to-noise ratio (SNR) performance for both nuclei is a desirable extension in order to gain greater insight into the physiological processes taking place in the brain together with their spatial localization and extent.

The double tuning of MRI coils has been implemented in various ways. The common approach is to extend an existing structure to support double resonances, e.g. four-ring birdcage coils [2-5] and alternating rungs in a birdcage [6], or to insert either active switching elements, e.g. PIN-diodes [7-9] and MEMS switches [10], or trap circuits [11-13]. Both enable a single physical structure to support two suitable resonant modes at different frequencies. An alternative solution is to implement two independent physical structures, each resonant at one of the desired frequencies. The latter approach requires coupling between the two structures to be minimized and various methods have been presented to achieve this, for example, nested coils [14-16], geometrical decoupling [17, 18], blocking traps [19, 20], PIN-diodes [21] or combinations of these mentioned above.

To date, most of the MR coils developed to overcome the challenges associated with simultaneous MR-PET imaging have either focused on providing low 511 keV gamma absorption or the RF coil has been installed outside the PET field-of-view (FoV). Examples of the latter include electrically floating RF screens of the PET cassettes with an external RF coil [22], the arrangement of the RF coil between the PET cassettes [23], and designs using scintillators arranged within the RF coil but using optical/electrical transmission to remote PET readout electronics [24, 25]. Low gamma-quanta absorption designs, where the PET ring is external to the RF coil, focus on removing the high absorbing circuitry from the PET FoV [26], a low absorption case design [27] and the optimization of the case geometry for both low absorption and good PET reconstruction properties [28]. In most cases, MR-PET compatible coils have only been designed as proton coils,

A. A. Celik is with the Institute of Neuroscience and Medicine – 11, Forschungszentrum Jülich, Jülich, Germany (a.celik@fz-juelich.de), C.-H. Choi (c.choi@fz-juelich.de), L. Tellmann (l.tellmann@fz-juelich.de), C. Rick (cl.rick@fz-juelich.de) and J. Felder (j.felder@fz-juelich.de) are with the Institute of Neuroscience and Medicine – 4, Forschungszentrum Jülich, Jülich, Germany. Corresponding to c.choi@fz-juelich.de or j.felder@fz-juelich.de.

N. J. Shah is with the Institute of Neuroscience and Medicine – 4, Forschungszentrum Jülich, Jülich, Germany, with the Institute of Neuroscience and Medicine – 11, Forschungszentrum Jülich, Jülich, Germany, with JARA - BRAIN - Translational Medicine, Aachen, Germany and with the Department of Neurology, RWTH Aachen University, Aachen, Germany (e-mail: n.j.shah@fz-juelich.de).

although, recently, double-tuned MR-PET coils have been investigated either by using standard MR coils [24] or by modifying a commercial double-tuned MR birdcage coil [29]. However, it must be noted that, the coil presented in [29] is unshielded and thus not suitable for operation in brain PET inserts which are physically close to the RF coil.

In this work, we present a double-tuned MR-PET volume head coil that has been optimized from the outset for operation inside a Brain PET insert [30] with the aim of investigating the trade-off encountered when balancing MR performance with multimodal imaging. The coil is designed to operate at both the proton frequency and the ^{31}P frequency of a 3 T MRI system and is primarily intended for oncology applications, e.g. to explore tumor extent using FDG-PET [31] and for the grading of gliomas with the aid of ^{31}P MR spectroscopy (MRS) [32]. PET performance was directly investigated with transmission scans at 511 keV, while the MR properties were investigated in simulations and phantom experiments and compared to a commercial, double-tuned birdcage coil intended for MR-only applications.

II. Materials and Methods

A. Overall design

The focus of the work was to create a double-tuned MR-PET coil with ultra-low gamma ray absorption and scatter properties, in order to maintain a high PET count efficiency and low SNR penalties on both the proton and the ^{31}P channel. Double-tuned coils can either employ birdcage like structures with traps/PIN-diodes or additional end rings to actively switch the resonance frequencies, or surface coil elements can be made double resonant by introducing a means to split normally mono-resonant structures. An overview of double-tuned MR coil structures is compiled in [33]. Here, because operation in both transmit and receive is desired, a birdcage design is preferred due to its ability to produce a homogenous field distribution. In addition, because of the limited space available in hybrid MR-PET environments targeting the human brain, designs that use two interleaved birdcage structures are the most space-efficient. However, they usually require the current flow of the proton frequency on the lower frequency structure to be blocked with the use of either trap circuits or PIN-diodes. In the design presented here, LC traps are implemented as these do not require a bias supply and allow coils to be operated at two frequencies simultaneously, e.g. if decoupling experiments are desired.

The constructed coil, without outer cases, is shown in Fig. 1. To reduce the number of lossy decoupling elements as much as possible, a separated, interleaved birdcage design was chosen with a minimum number of traps on the lower frequency rungs. For sake of simplicity, the traps are implemented as LC traps, although higher SNRs can be obtained with alternative trap circuits [34]. However, in order to maintain the highest possible SNR with this trap configuration, a low value of 33 nH was selected for the trap inductor.

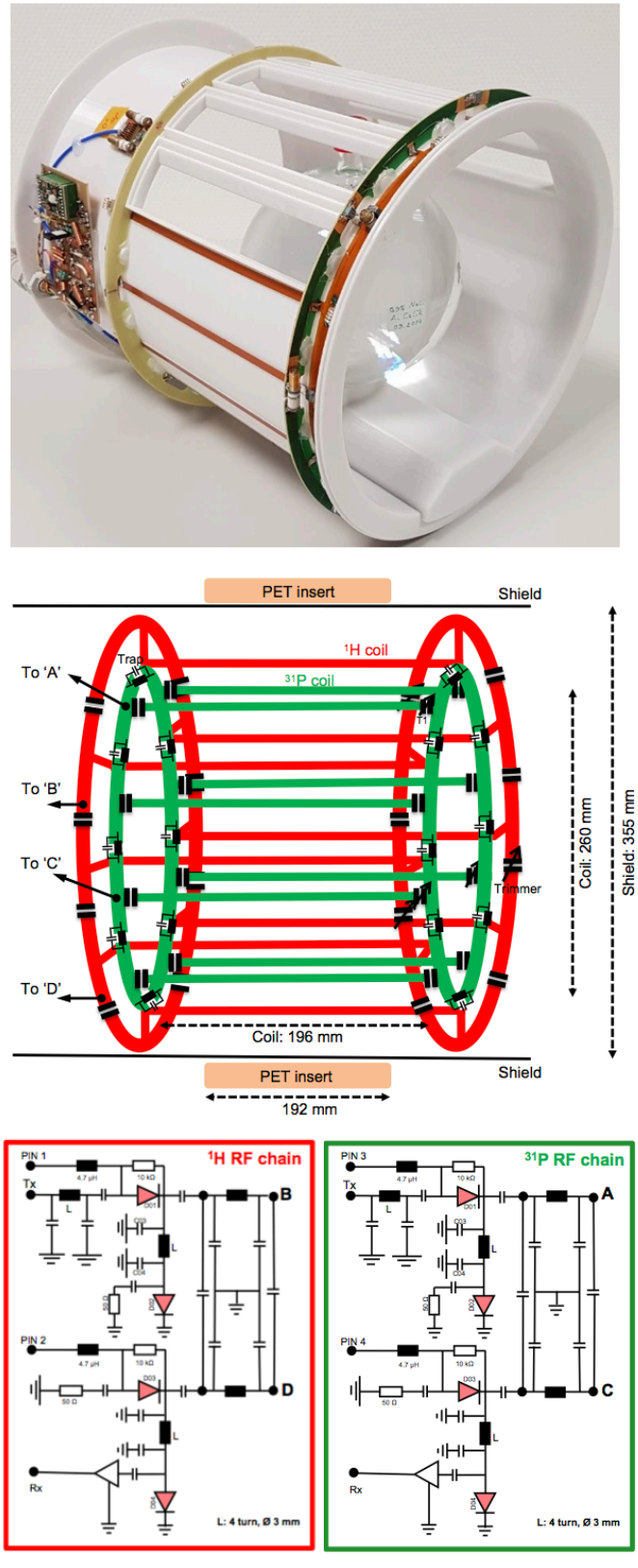

Fig. 1 The double resonant head coil without the outer cover (top), schematic of the coil including orientation inside the PET FoV (middle) and T/R circuitry for both the ^{1}H and ^{31}P channel (bottom). A low-pass design is used for the ^{31}P coil and a high-pass design is used for the ^{1}H element. Each of the two individual birdcages is based on an eight-rung geometry and is driven in quadrature. The lengths of the ^{1}H and ^{31}P rungs are 196 mm and 222 mm, respectively. The width of the end ring traces is 8 mm.

To reduce the required space for the two end rings, and to facilitate geometrically simple junctions between the two separate resonator structures, each end ring of the ^{1}H coil is folded upright similar to [4]. The coil is designed to cover the whole head, with a free inner diameter of 260 mm. In order to fit in the 'BrainPET' PET detector ring (Siemens Healthineers, Erlangen, Germany), the outer diameter of the coil is fixed to 330 mm. The coil system uses a low-pass design for the ^{31}P antenna and a high-pass for the ^{1}H element, resulting in realizable capacitor values for both systems (compare [35]). Each of the two individual birdcages is based on an eight-rung geometry and is driven in quadrature. As there is no interference between the modes of the ^{1}H and ^{31}P systems, the design is electrically similar to the multinuclear MR-PET coil described in [29]. However, the birdcages in the implementation presented here need to be considered as shielded, as they are intended to operate inside the BrainPET insert, which acts as an RF screen for the MR coil.

B. Case material and geometry

To be able to produce a case with the complex geometry required to reduce PET attenuation arising from variations in material thickness, additive manufacturing methods were investigated for case production. Materials compatible with the 3D printer available on-site (Fortus 400mc, Stratasys Inc., Eden Prairie, USA) have previously been tested for MR compatibility [44], and polycarbonate was found to be a suitable candidate – which was also used in an earlier MR-PET coil [26]. However, in order to achieve sufficient mechanical sturdiness and electrical isolation required to comply with the IEC 60601-1 guideline in the proposed design, a minimum wall thickness of 4 mm was maintained, as compared to only 2.7 mm in the above reference. Coating of the polycarbonate was required to make the 3D printed case impermeable to water. However, some coatings are highly absorbing to PET irradiation [28]. As a possible solution, the use of a plastic coating was investigated and adcoat® (Adelhelm Kunststoffbeschichtungen GmbH, Eningen, Germany) was found to be a suitable candidate. This particular coating has the advantage of being compatible with food production and thus, is highly likely to be biocompatible. PET compatibility of the 3D printed polycarbonate and coating was verified with transmission scans and the results are shown in Fig. 2. MR compatibility of both materials was validated as described above. MR images from the B_0 compatibility and proton signal tests are shown in Fig. 3.

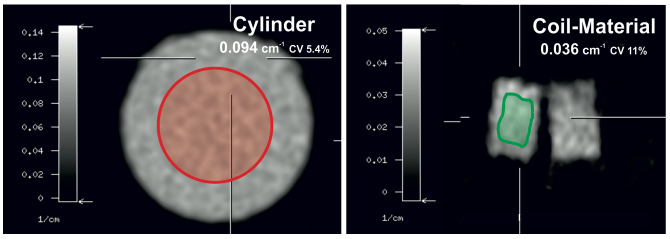

Fig. 2 ROI analysis of the attenuation maps from a homogenous water filled cylinder (left) and coil material (right). The figure shows that the printed polycarbonate case and coating had a very low impact on PET performance.

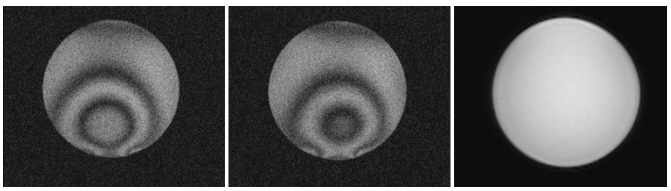
Fig. 3 B_0 field interference pattern without plastic casing and shim currents set to zero (left) and after inserting a coated plastic sample (middle). Proton image from the phantom without visible signal from the case (right).

C. PET compatibility issues

In order to make the complete coil assembly as PET transparent as possible, several design aspects required special attention. These included: 1) the removal of all high 511 keV gamma absorbing components from the PET FoV, 2) the use of low 511 keV gamma absorbing electrical conductors to limit the impact of losses caused by the RF coil as much as possible, and 3) the optimization of the coil casing for low gamma absorption. For the sake of clarity, the center of the PET FoV coincides with the center of the rungs and extends to 196 mm in the axial direction.

The first issue is straightforward and has been extensively discussed in the literature, e.g. [26]. In the particular implementation presented here, all electrical connections to the coil system are carried out from the rear of the magnet so that all electrical circuits required for its operation (transmit/receive (T/R) switches, hybrids, frequency diplexer, preamplifiers, transmission lines, cable traps, etc.) are arranged towards the far end of the coil and outside the PET FoV. As the ^{1}H high-pass only requires capacitors to be placed on the end rings, there are no lumped components in the PET FoV. For the ^{31}P low-pass coil, the capacitors required on the birdcage rungs have been split into two series capacitors for each rung and are geometrically arranged on both ends of the rung. This has been described in [14] and effectively removes the low-pass capacitors from the PET FoV. The eight proton trap circuits located on both ^{31}P end rings stop the coupling of the proton signal onto the ^{31}P system and result in an added inductance to the end ring segments at the ^{31}P frequency. The capacitors on the coil are fixed, non-magnetic chip capacitors (25 case size series, Voltronics corp., Denville, USA), and, for the sake of simplicity, tuning and matching was carried out using variable capacitors (NMA_HV series, Voltronics corp., Denville, USA). The circuit diagrams of both coil systems are shown in Fig. 1.

The second issue has been investigated in [36] and a suitable compromise between PET attenuation and RF electric losses is the use of thin and narrow copper traces (thickness: 35 µm). Here, the coil uses 5 mm wide copper traces for the rungs and an 8 mm trace width for the end rings. All traces are etched on a flexible PCB on a polyimide substrate (KREMPEL GmbH, Vaihingen, Germany) which is fixed to the 3D printed coil case using adhesive tape (3M, Maplewood, USA). Exceptions are the folded end rings, placed outside the PET FOV, which use 1.5 mm thick standard FR4 based PCBs for mechanical stability.

In terms of the third point, the case material and the case varnish were selected to provide mechanical stability and

suitable electrical insulation while exhibiting low PET absorption and negligible MR signal at the $^{1}H/^{31}P$ frequencies. The paint, which comes into contact with the patient, was also required to be bio-compatible as per normative requirements [37]. The goal for the selection of appropriate materials was a lower 511 keV absorption than that of water – which is comparable to the absorption encountered in the RF coil for the BrainPET insert [28]. Materials were evaluated by transmissions scans inside an ECAT HR+ PET scanner (Siemens Healthineers, Erlangen, Germany). The MR compatibility of the materials (no signal from the case and no static magnetic field (B_0) distortions) was either confirmed from prior publications or by measurements of representative samples on a small animal scanner [38]. The setup used a spherical water phantom of 40 mm diameter (0.0444 g $MnCl_2$ + 0.0667 g NaCl per 1000 g distilled water) placed on top of the sample material and two different MR sequences. B_0 distributions with the sample present were compared to those without the sample with the help of a 2D spin-echo sequence using a regular and stimulated echo to encode the B_0 distribution in an interference pattern (repetition time (TR) = 300 ms, interference stripe distance of 100 Hz, flip angles (FA) = 90/130/130°, FOV = 60 mm × 60 mm, matrix size = 256 × 256, slice thickness = 1 mm). The signal from the sample material was measured using a fast 3D gradient-echo sequence (TR = 20 ms, TE = 0.59 ms, FA = 25°, FOV = 60 mm × 60 mm, matrix size = 128 × 128, slice thickness = 1 mm, NEX = 1, TA = 52 s). Finally, as required by [28], the case design is such that it avoids sharp changes in the radial attenuation profile as well as paths with high amounts of material.

D. MR related performance evaluation

Initial evaluation of the coil was performed on the bench with the coil being loaded with a spherical phantom (inner diameter: 165 mm, filled with 2 liters of distilled water doped with 1.24 g $NiSO_4 \times 6\ H_2O$, 2.62 g NaCl and 2 g KH_2PO_4 per liter) inside a dummy shield identical to the RF screen of the BrainPET insert. Measurements taken included input matching of both coil systems and loaded to unloaded quality (Q) factor ratios. Q factors were acquired as described in [39]. All measurements were carried out using a ZVL series network analyzer (Rhode & Schwarz, München, Germany).

The RF coil was evaluated against an unshielded, commercially available $^{1}H/^{31}P$ double resonant coil – similar to the one described in [29] but without being optimized for PET compatibility. Comparisons were done in terms of specific absorption rate (SAR) burden and imaging/spectroscopic performance.

For this purpose, the B_1^+ transmit efficiency and SAR burden of the proposed coil system was evaluated at the two Larmor frequencies with the aid of numerical simulations using the finite integration technique, as implemented in the CST simulation suite (CST AG, Darmstadt, Germany), and a head voxel model [40]. These values were then compared with the values obtained through identical simulations of the commercial 8-rung, double-tuned coil (RAPID Biomedical GmbH, Rimpar, Germany). The geometry of the commercial coil was reconstructed in the simulator from CT scans of the physical coil.

Proton images and ^{31}P spectra were acquired using the phantom described above on a 3 T TRIO system (Siemens Healthineers, Erlangen, Germany) with both the proposed and commercial RF coils. The corresponding Larmor frequencies of ^{1}H and ^{31}P at 3 T are 123.2 MHz and 49.9 MHz, respectively. The RF transmit power was calibrated and optimized by applying a range of RF power which required the same transmit power for both the proposed and commercial double-tuned coils. Proton images were acquired with a single slice gradient-echo sequence (TR = 800 ms, TE = 2.33 ms, NEX = 1, slice thickness = 5 mm, FA = 30°, FOV = 250 mm × 250 mm, matrix size = 128 × 128, TA = 2:33 minutes) in the isocenter and were also used for the SNR measurements of the proton channel. SNR was computed by dividing the signal mean of the phantom area by the noise standard deviation measured with the transmit power set to zero (method 2 in [41]) and accounting for magnitude image reconstruction. Additional experiments were conducted to obtain images acquired using turbo spin-echo and B_1 maps acquired using a double-angle method in order to support the comparison (See Fig. S2 and Fig. S3, respectively). ^{31}P spectra were acquired using a chemical shift imaging sequence (TR = 2 s, TE = 2.3 ms, NEX = 1, voxel size = 30 mm × 30 mm × 30 mm with weighted phase encoding, TA = 4:07 minutes) to calculate the SNR for the phosphorous channel and to evaluate the homogeneity of the birdcages. All ^{31}P data were processed and SNRs, the signal mean value divided by the standard deviation in residual noise, were calculated with jMRUI software [42], using the advanced method for accurate, robust and efficient spectral fitting [43]. The MR results were compared with those of a commercial double-tuned coil. Importantly, all measurements using the MR-PET coil system developed here required the installation of a dummy RF screen, which mimics the shield of the Brain PET insert.

E. PET related performance evaluation

A dedicated PET scanner (ECAT EXACT HR+, Siemens Healthineers, Erlangen, Germany) equipped with rotating $^{68}Ge/^{68}Ga$ rod sources (each around 150 MBq) was used to measure the attenuation characteristics of the coil at 511 keV. Measurements were performed over 10 hours in order to obtain high count rate statistics. Data were reconstructed with OSEM2D (6 iterations, 16 subsets, no filtering) with a matrix size of 256 × 256 and 154 slices, resulting in a pixel size of 2.57 mm × 2.57 mm and a slice thickness of 2.57 mm.

III. RESULTS

Table I. Measured Q-factors of the proposed double-tuned coil

	Q_{Un}	Q_L	Q_{Un}/Q_L
^{1}H	230	72	3.2
^{31}P	310	122	2.5

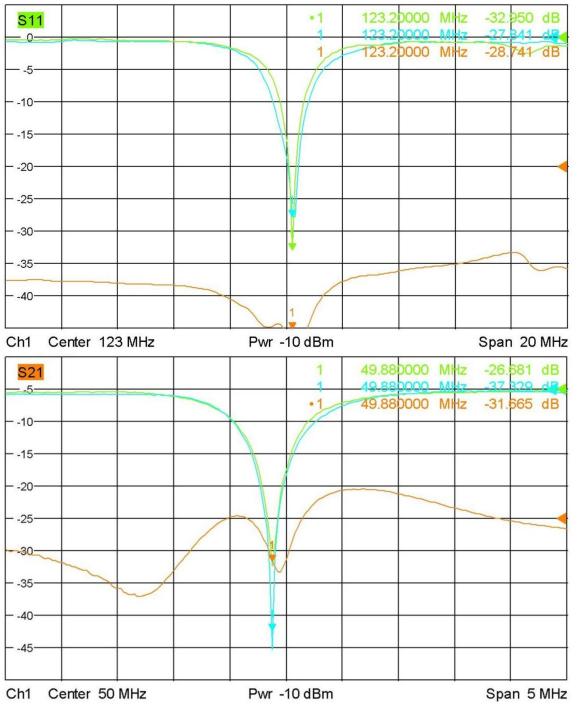

Fig. 4 Tuning and matching of the proposed double-tuned coil (0°: green, 90°: blue) and isolation between 0 and 90° channels (orange) for the proton system (top) and phosphorous system (bottom). It can be seen that, in all cases, matching is better than -27 dB and isolation is more than 28 dB.

A. MR related performance

Fig. 4 shows the measured input reflection of both quadrature ports as well as the isolation between them. Measurements for the proton channel are shown in the top row and those for the ^{31}P channel are shown in the bottom row. In all cases, matching is better than -27 dB and isolation is more than 28 dB. The measured quality factors are given in Table I.

The simulation setup for the evaluation of the specific absorption rate is shown in Fig. 5. The B_1^+ distribution and 10 g averaged SAR burden, normalized to 1 W accepted power for the ^{1}H and ^{31}P systems, are shown in the sagittal slices below. An average $|B_1^+|$ of 0.672 µT/√1 W was numerically computed for the PET compatible coil and a value of 0.634 µT/√1 W was computed for the commercial coil at the proton frequency. The values for the ^{31}P nucleus are 1.88 µT/√1 W and 1.90 µT/√1 W, respectively. Thus, with the power amplifiers available in the system, a target $|B_1^+|$ of 20 µT can be reached for both nuclei and with both coil systems.

On the proton frequency, the PET-compatible coil system is limited by its local SAR, allowing a long term averaged transmit power of 11.2 W, while the commercial coil is limited by the head SAR with a permissible power of 17.0 W averaged over 6 min. For the ^{31}P frequency, SAR limits are 13.6 W (local SAR limit) and 14.8 W (global SAR limit), respectively. Detailed information on these values can be found in Supplemental Table S1.

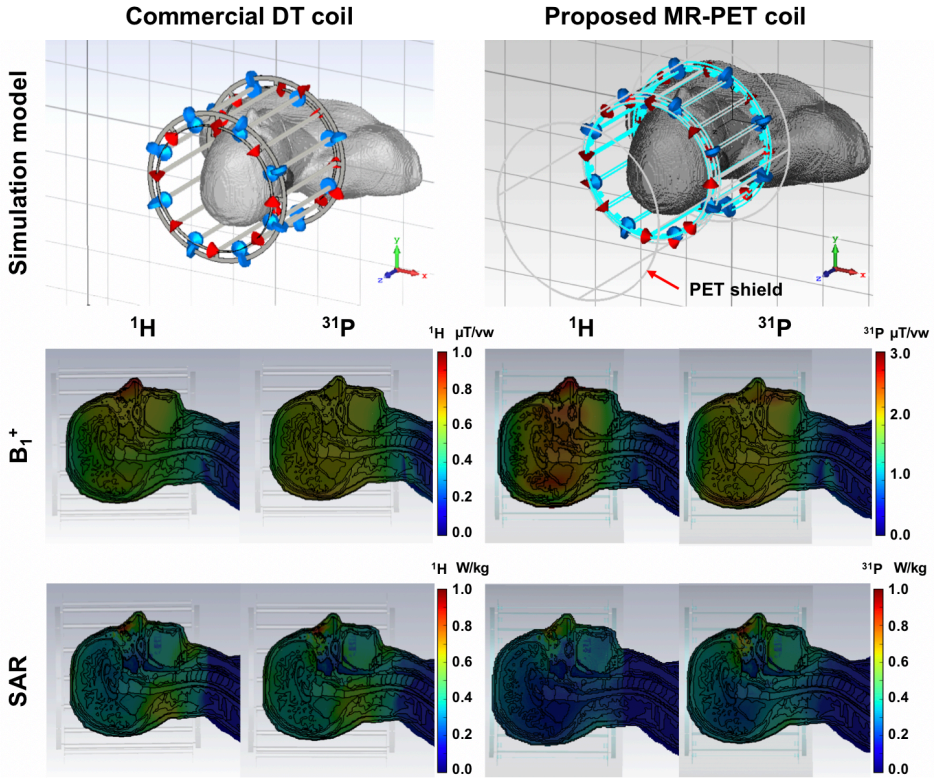

Fig. 5 The simulation models of commercial double-tuned coil and the proposed double-tuned MR-PET coil (top row). Each model was used for the evaluation of the B_1^+ distribution (middle row) and the specific absorption rate (bottom row). 10 g averaged SAR burden was normalized to 1 W accepted power for the ^{1}H and ^{31}P channel of both systems and the sagittal slices are shown.

Fig. 6 compares the SNR values for the proposed coil with those of the commercially available coil, acquired in the same scanner. However, in contrast to the commercially available coil, the coil developed here was RF shielded by the PET ring. As can be seen, despite the tight-fitting RF screen on the proposed coil, which reduces the coil's sensitivity (compare Supplemental Fig. S1), the calculated proton SNR is higher than that of the commercially available coil. The same holds for the SNR obtained with spectroscopic measurements for the ^{31}P channels of both coils as shown in Fig. 7. The maximum SNR values were 9.29 vs. 6.81 for the proposed coil and the commercially available coil, respectively.

B. PET related performance

The count rate loss with the proposed coil inside the BrainPET insert was 5.2%, while this value for the commercially available coil was 9.3%. Fig. 8 shows the attenuation maps acquired with transmission scans for both coil systems in three orthogonal cross sections.

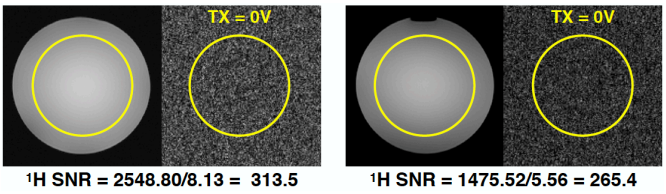

Fig. 6 Comparison of ^{1}H SNR values – proposed coil (left) and commercial coil (right). The calculated proton SNR is higher than that of the commercially available coil, despite the tight fitting.

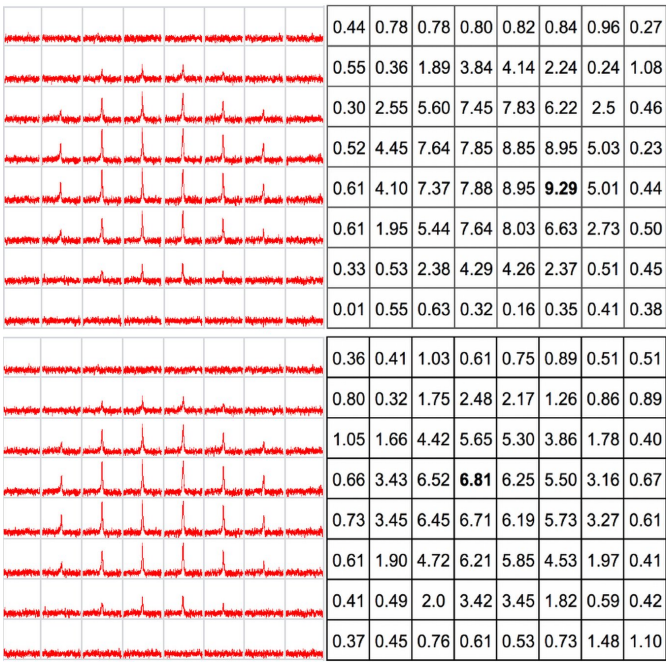

Fig. 7 ^{31}P spectra (left) with the calculated SNR values (right) – proposed coil (top, max: 9.29) and the commercial coil (bottom, max: 6.81). As can be seen, the maximum SNR values were 9.29 for the proposed coil and are, on average, higher than those of the commercially available coil.

IV. Discussion and Conclusions

This work demonstrates the successful implementation of a double-tuned coil suitable for use in an integrated head MR-PET system. The results show that this coil can be operated at both resonance frequencies without SNR degradation of the MR signal and with only a negligible penalty on the PET count rate loss. The key factor for good performance in both modalities is to find suitable compromises for low gamma absorbing materials without significantly increasing the associated RF losses. In the case presented here, the major benefits result from an optimized geometric layout, the choice of case materials and the careful selection of coil conductor materials and thicknesses. By applying the aforementioned principles, the double resonant MR coil exhibited an overall count rate loss of 5.2%, which is better than that reported in [24, 27], where count rate losses of 17% and 9.1% were given. Also, despite reports on increased radiation doses in LINAC systems when inserting copper traces [46], the PCB traces of 35 µm thickness did not contribute to significant PET attenuation in our case. This is also why no attempts were made to use a conductor material with lower absorption, such as aluminum. Moreover, several reports indicate significant SNR degradation when aluminum is used, e.g. [26, 46].

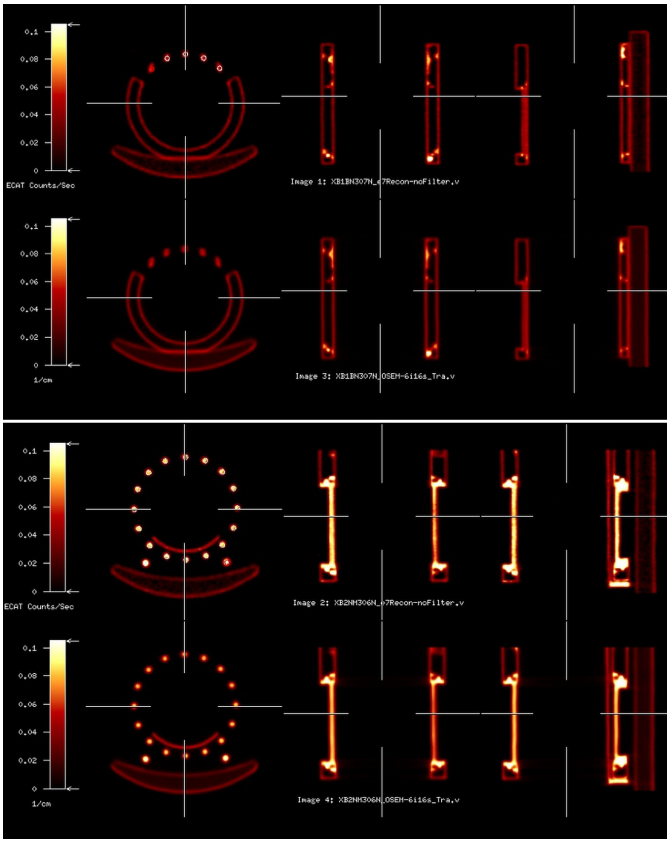

Fig. 8 Attenuation maps of the proposed coil system (top) and the commercial, double-tuned birdcage coil (bottom) in three orthogonal cross sections. The count rate loss with the proposed coil inside the BrainPET insert was 5.2%, compared to 9.3% for the commercially available coil.

The MR performance of the proposed coil system has been demonstrated to be comparable to or better than that of a similar, commercially-available, double-tuned coil. Moreover, this is true, even though the PET compatible design operates in the RF screened environment of the PET insert and screening is known to reduce SNR in MR experiments. It is expected that, when used with a PET screen, the commercially-available coil would show worse performance figures than those reported here without a screen.

Overall, the investigations performed here show that the coil system is well suited to a MR-PET system without causing significant performance degradations in either modality. Moreover, in MR operation, it provides high SNR for both nuclei, which is a crucial design goal, even when building MR-only, double-tuned coil systems. Having demonstrated good performance in phantom investigations, the next step is to obtain clearance for in vivo investigations.

References

[1] W. A. Worthoff, A. Shymanskaya, C.-H. Choi, J. Felder, A.-M. Oros-Peusquens, and N. J. Shah, "Multinuclear MR Imaging and Spectroscopy," in *Quantitative MRI of the Brain.*, M. Cercignani, N. Dowell, and P. Tofts Eds., 2nd ed. Boca Raton: CRC Press, 2018, ch. 13.

[2] Y. Duan, B. S. Peterson, F. Liu, T. R. Brown, T. S. Ibrahim, and A. Kangarlu, "Computational and experimental optimization of a double-tuned (1)H/(31)P four-ring birdcage head coil for MRS at 3T," *J. Magn. Reson. Imag.,* vol. 29, no. 1, pp. 13-22, 2009.

[3] J. R. Fitzsimmons, B. L. Beck, and H. R. Brooker, "Double resonant quadrature birdcage," *Magn. Reson. Med.,* vol. 30, no. 1, pp. 107-14,1993.

[4] Y. Ha *et al.*, "Design and use of a folded four-ring double-tuned birdcage coil for rat brain sodium imaging at 9.4 T," *J. Magn. Reson.,* vol. 286, pp. 110-114, 2018.

[5] J. Murphy-Boesch, R. Srinivasan, L. Carvajal, and T. R. Brown, "Two configurations of the four-ring birdcage coil for 1H imaging and 1H-decoupled 31P spectroscopy of the human head," *J. Magn. Reson.,* vol. 103, no. 2, pp. 103-14, 1994.

[6] S. Amari, A. M. Ulug, J. Bornemann, P. C. van Zijl, and P. B. Barker, "Multiple tuning of birdcage resonators," *Magn. Reson. Med.,* vol. 37, no. 2, pp. 243-51, 1997.

[7] C. H. Choi, S. M. Hong, Y. Ha, and N. J. Shah, "Design and construction of a novel 1H/19F double-tuned coil system using PIN-diode switches at 9.4T," *J. Magn. Reson.,* vol. 279, pp. 11-15, 2017.

[8] C. H. Choi, J. M. Hutchison, and D. J. Lurie, "Design and construction of an actively frequency-switchable RF coil for field-dependent Magnetisation Transfer Contrast MRI with fast field-cycling," *J. Magn. Reson.,* vol. 207, no. 1, pp. 134-9, 2010.

[9] S. Ha, M. J. Hamamura, O. Nalcioglu, and L. T. Muftuler, "A PIN diode controlled dual-tuned MRI RF coil and phased array for multi nuclear imaging," *Phys. Med. Biol.,* vol. 55, no. 9, pp. 2589-600, 2010.

[10] A. Maunder, M. Rao, F. Robb, and J. M. Wild, "Comparison of MEMS switches and PIN diodes for switched dual tuned RF coils," *Magn. Reson. Med.,* vol. 80, no. 4, pp. 1746-1753, 2018.

[11] G. Isaac, M. D. Schnall, R. E. Lenkinski, and K. Vogele, "A design for a double-tuned birdcage coil for use in an integrated MRI/MRS examination," *J. Magn. Reson.,* vol. 89, no. 1, pp. 41-50, 1990.

[12] M. D. Schnall, V. H. Subramanian, J. S. Leigh, and B. Chance, "A new double-tuned probe for concurrent H-1 and P-31 NMR," *J. Magn. Reson.,* vol. 65, no. 1, pp. 122-129, 1985.

[13] G. X. Shen, F. E. Boada, and K. R. Thulborn, "Dual-frequency, dual-quadrature, birdcage RF coil design with identical B1 pattern for sodium and proton imaging of the human brain at 1.5 T," *Magn. Reson. Med.,* vol. 38, no. 5, pp. 717-25, 1997.

[14] A. Asfour, "Design and development of a new dedicated RF sensor for the MRI of rat brain," *J. Biomed. Sci. Eng.,* vol. 3, no. 2, p. 14, 2010.

[15] R. Brown *et al.*, "A flexible nested sodium and proton coil array with wideband matching for knee cartilage MRI at 3T," *Magn. Reson. Med.,* vol. 76, no. 4, pp. 1325-34, 2016.

[16] R. Brown, K. Lakshmanan, G. Madelin, and P. Parasoglou, "A nested phosphorus and proton coil array for brain magnetic resonance imaging and spectroscopy," *NeuroImage,* vol. 124, pp. 602-611, 2016.

[17] G. Adriany and R. Gruetter, "A half-volume coil for efficient proton decoupling in humans at 4 tesla," (in English), *J. Magn. Reson.,* vol. 125, no. 1, pp. 178-84, 1997.

[18] M. P. McDougall, S. Cheshkov, J. Rispoli, C. Malloy, I. Dimitrov, and S. M. Wright, "Quadrature transmit coil for breast imaging at 7 Tesla using forced current excitation for improved homogeneity," *J. Magn. Reson Imag.,* vol. 40, no. 5, pp. 1165-73, 2014.

[19] M. Alecci, S. Romanzetti, J. Kaffanke, A. Celik, H. P. Wegener, and N. J. Shah, "Practical design of a 4 Tesla double-tuned RF surface coil for interleaved H-1 and Na-23 MRI of rat brain," *J. Magn. Reson.,* vol. 181, no. 2, pp. 203-211, 2006.

[20] G. B. Matson, P. Vermathen, and T. C. Hill, "A practical double-tuned H-1/P-31 quadrature birdcage headcoil optimized for P-31 operation," *Magnet. Reson. Med.,* vol. 42, no. 1, pp. 173-182, 1999.

[21] Y. Ha, C. H. Choi, and N. J. Shah, "Development and implementation of a PIN-diode controlled, quadrature-enhanced, double-tuned RF coil for sodium MRI," *IEEE Trans. Med. Imag.,* vol. 37, no. 7, pp. 1626-1631, 2018.

[22] A. M. Grant, B. J. Lee, C. M. Chang, and C. S. Levin, "Simultaneous PET/MR imaging with a radio frequency-penetrable PET insert," *Med. Phys.,* vol. 44, no. 1, pp. 112-120, 2017.

[23] M. S. H. Akram *et al.*, "MRI compatibility study of an integrated PET/RF-coil prototype system at 3T," *J. Magn. Reson.,* vol. 283, pp. 62-70, 2017.

[24] N. Omidvari, G. Topping, J. Cabello, S. Paul, M. Schwaiger, and S. I. Ziegler, "MR-compatibility assessment of MADPET4: a study of interferences between an SiPM-based PET insert and a 7 T MRI system," *Phys. Med. Biol.,* vol. 63, no. 9, pp. 23, 2018,

[25] N. J. Shah, *Hybrid MR-PET Imaging* (New Developments in NMR). 2018.

[26] C. Y. Sander, B. Keil, D. B. Chonde, B. R. Rosen, C. Catana, and L. L. Wald, "A 31-channel MR brain array coil compatible with positron emission tomography," *Magn. Reson. Med.,* vol. 73, no. 6, pp. 2363-75, 2015.

[27] G. Delso *et al.*, "Evaluation of the attenuation properties of MR equipment for its use in a whole-body PET/MR scanner," *Phys. Med. Biol.,* vol. 55, no. 15, pp. 4361-4374, 2010.

[28] C. W. Lerche *et al.*, "PET attenuation correction for rigid MR Tx/Rx coils from (176)Lu background activity," *Phys. Med. Biol.,* vol. 63, no. 3, p. 035039, 2018.

[29] M. Oehmigen *et al.*, "A dual-tuned (13) C/(1) H head coil for PET/MR hybrid neuroimaging: Development, attenuation correction, and first evaluation," *Med. Phys.,* vol. 45, no. 11, pp. 4877-4887, 2018.

[30] A. Kolb *et al.*, "Technical performance evaluation of a human brain PET/MRI system," *Eur. Radiol.,* vol. 22, no. 8, pp. 1776-88, 2012.

[31] K. J. Langen, N. Galldiks, E. Hattingen, and N. J. Shah, "Advances in neuro-oncology imaging," *Nat. Rev. Neurol.,* vol. 13, no. 5, pp. 279-289, 2017.

[32] J. Novak, M. Wilson, L. Macpherson, T. N. Arvanitis, N. P. Davies, and A. C. Peet, "Clinical protocols for 31P MRS of the brain and their use in evaluating optic pathway gliomas in children," *Eur. J. Radiol,* vol. 83, no. 2, pp. 106-12, 2014.

[33] C.-H. Choi, S.-M. Hong, J. Felder, and N. J. Shah, "The state-of-the-art and emerging design approaches of double-tuned RF coils for X-nuclei, brain MR imaging and spectroscopy: A review," *Magn. Reson. Imag.,* vol. 72, pp. 103-116, 2020.

[34] M. Meyerspeer, E. S. Roig, R. Gruetter, and A. W. Magill, "An improved trap design for decoupling multinuclear RF coils," *Magnet. Reson. Med.,* vol. 72, no. 2, pp. 584-590, 2014.

[35] A. M. Hudson, W. Kockenberger, and R. W. Bowtell, "Dual resonant birdcage coils for 1H detected 13C microscopic imaging at 11.7 T," *MAGMA,* vol. 10, no. 2, pp. 61-8, 2000.

[36] C.-H. Choi, L. Tellmann, J. Felder, C. Lerche, and N. J. Shah, "An evaluation of RF coil materials for 1H/31P for use in a hybrid MR-PET scanner at 3T," in *Proceedings 25th Scientific Meeting, International Society for Magnetic Resonance in Medicine*, Hawaii, April 2017, p. 4432.

[37] *Medical electrical equipment - Part 1: General requirements for basic safety and essential performance*, I. E. Commission, Geneva, Switzerland, 2012.

[38] J. Felder, A. A. Celik, C. H. Choi, S. Schwan, and N. J. Shah, "9.4 T small animal MRI using clinical components for direct translational studies," *J. Transl. Med.,* vol. 15, no. 1, p. 264, 2017.

[39] A. Kumar, W. A. Edelstein, and P. A. Bottomley, "Noise figure limits for circular loop MR coils," *Magn. Reson. Med.,* vol. 61, no. 5, pp. 1201-9, 2009.

[40] A. Christ *et al.*, "The Virtual Family--development of surface-based anatomical models of two adults and two children for dosimetric simulations," *Phys. Med. Biol.,* vol. 55, no. 2, pp. 23-38, 2010.

[41] *Determination of Signal-to-Noise Ratio (SNR) in Diagnostic Magnetic Resonance Imaging*, 100123, NEMA, April 30th, 2015. [Online]. Available: https://www.nema.org/Standards/Pages/Determination-of-Signal-to-Noise-Ratio-in-Diagnostic-Magnetic-Resonance-Imaging.aspx

[42] A. Naressi, C. Couturier, I. Castang, R. de Beer, and D. Graveron-Demilly, "Java-based graphical user interface for MRUI, a software package for quantitation of in vivo/medical magnetic resonance spectroscopy signals," *Comput. Biol. Med.,* vol. 31, no. 4, pp. 269-286, 2001.

[43] L. Vanhamme, A. van den Boogaart, and S. Van Huffel, "Improved method for accurate and efficient quantification of MRS data with use of prior knowledge," *J. Magn. Reson.,* vol. 129, no. 1, pp. 35-43, 1997.

[44] "MRI scanners: Evaluation of the Compatibility of FDM Materials in High Field Strength Fields," Startasys Inc., 2011. Accessed: 10.01.2019. [Online]. Available: http://usglobalimages.stratasys.com/Main/Secure/Applications/End%20Use%20Parts/Technical%20application%20guide%20-%20MRI%20scanners.pdf?v=635533848469537913

[45] U. C. Anazodo *et al.*, "Assessment of PET performance of a 32-Channel MR Brain Array Head Coil Compatible with PET for Integrated PET-MRI," in *Proc. 7th conference on PET/MR and SPECT/MR*, 2016, vol. 7.

[46] R. Barta, A. Ghila, S. Rathee, B. G. Fallone, and N. DeZanche, "Low-attenuation RF surface coils for LINAC:-MR hybrids: Comparison between radiation dose to skin and SNR," in *Proceedings 25th Scientific Meeting, International Society for Magnetic Resonance in Medicine, Honululu*, 2017, pp. 2978-2978.